Biophysical Chemistry, 45 (1992) 101–108
Elsevier Science Publishers B.V., Amsterdam

BIOCHE 01701

Light scattering of DNA plasmids containing repeated curved insertions: Anomalous compaction

Giuseppe Chirico, Sabrina Beretta and Giancarlo Baldini
Universita' degli Studi di Milano, Dipartimento di Fisica, Via Celoria 16, 20133-I (Italy)

(Received 30 March 1992; accepted in revised form 8 July 1992)

Abstract

The plasmid pUC18m containing the insertion of the curved sequence AluI, repeated from one to six times, has been studied by dynamic light scattering. The values of the translational diffusion coefficient D_t for the whole series of inserted plasmids show oscillating behaviour versus the length of the insertion and two plasmids, those containing two and six AluI adjacent sequences, respectively, display a remarkable compaction. The occurrence of either an interwound linear structure or an interwound branched form for the inserted plasmids is discussed and tested by employing also a "string of beads" model that gives values of D_t in agreement with the observations.

Keywords: Curved DNA; Plasmid DNA; Dynamic light scattering; DNA conformation

1. Introduction

DNA may be found in two major forms inside the cell: the so called interwound and solenoidal conformations. Negative supercoiling is the common characteristic of these forms arising from given topological constraints, such as the attachment of the two ends of a double helix to a protein matrix [1,2], or the closure of DNA in a plasmid. The interwound form is composed of two DNA double helices belonging to the same portion of the molecule and interwinding around each other to form an almost linear structure. This form, which is known to compact DNA poorly, two and half-fold, compared to the nine-fold compaction of the eukaryotic nucleosomes, seems very efficient in allowing fine regulation mechanisms [3]. In fact negative supercoiling helps processes which require untwisting or denaturation of part of a double helix such as those occuring during replication and transcription [4]. Furthermore the degree of supercoiling is kept at the physiological level ($\sigma \cong -0.025$) mainly by DNA interactions with several enzymes (topoisomerases) [5].

The solenoidal winding seen in eukaryotic nucleosomes [2] is highly efficient in packaging the DNA within the close confines of the nucleus. The DNA structure in nucleosomes has been largely attributed to the binding to histonic proteins, but several studies [6] have also shown the influence of DNA curvature. In fact the position

Correspondence to: Dr. G. Baldini, Universita' degli Studi di Milano, Dipartimento di Fisica, Via Celoria 16, 20133-1 (Italy).

of nucleosomes has been correlated with the presence of some short curved DNA tracts [6]. Furthermore, more and more curved sequences have being reported in the regulating regions of some genes [7,8], suggesting that DNA curvature has a relevant role in the activity of DNA.

Here we have observed, by dynamic light scattering (DLS) of DNA solutions, the conformational changes in small (ca. 3000 base pairs) plasmids with a varying number of inserted curved sequences. It has been demonstrated by Barigozzi et al. [9] that in *Artemia Franciscana* the heterochromatic DNA is actually composed of a highly repetitive (6×10^5 copies per haploid genome) AluI fragment of 113 bp in length particularly rich in AT content ($\cong 70\%$.) Studies of electrophoretic mobilities of N AluI contiguous fragments, ($N = 1, \ldots, 6$), have shown an anomalous mobility for this sequence [10] which has been attributed to an intrinsic DNA curvature as suggested by several groups [11].

In this paper we have studied the hydrodynamic properties of a plasmid, pUC18m, containing repeated AluI sequences in order to bring into evidence any conformational change in the host plasmid versus the length of the curved insertions ($N = 1, 2, \ldots, 6$)

2. Materials and methods

2.1 DNA purification

The plasmid DNAs were derived from pUC18m with the insertion of a different number of adjacent AluI monomeric units. The multimeric fragments were cloned in pUC18m by Badaracco et al. as previously described [10]. The plasmid containing N AluI adjacent sequences is denoted here P_N with $1 \leq N \leq 6$. The number of base pairs in pUC18m and AluI sequence is 2686 and 113, respectively. The plasmids were replicated by harbouring in *E. Coli* HB101 and prepared by lysozyme/SDS lysis and poly(ethylene glycol) (PEG) precipitation. The crude DNA has been purified by HPLC [12]. DNA has been checked on agarose gel electrophoresis and none of the samples was less than 90% superhelical DNA.

For DLS experiments DNA was dissolved in phosphate buffer (10 mM KH_2PO_4, 30 mM Na_2HPO_4, 0.1 mM Na_3-EDTA; pH 7.45, ionic strength $I = 100$ mM) and used at DNA phosphate concentration of 110–140 μM. The DNA solutions were filtered through 0.22 μm Millipore Durapore filters directly in the measurement cuvette in order to minimize dust contamination. All samples have been checked by circular dichroism measurements which revealed B-like spectra. After each series of DLS measurement which lasted 10–12 h, at temperature of 25°C, all the samples were checked for integrity by electrophoresis on 1% agarose gel. In no case superhelical DNAs were appreciably degraded to nicked circular or linear form.

2.2 Photon counting equipment

The light source is a vertically polarized Spectra-Physics He–Ne laser (25 mW) and the light scattered from a cylindrical cell is collected by an EMI 9863 KB photomultiplier. The output pulses are discriminated and sent to a Brookhaven Instruments BI-2030AT 4-bits digital correlator with 136 real-time channels for the autocorrelation function (ACF) computation. The correlator is always used in the multiple sample time option and the collection software has been modified in order to introduce a electronic "dust" filter [13]. This control program allows the collection of a prechosen number of ACFs rejecting those for which the calculated baseline (from the total photon count) differs from the measured baseline (from the last delay channels) by more than 0.5–0.8%. Each ACF was collected for 3–20 s and the total number of ACFs was chosen in order to have a baseline $\geq 100\,000$ photoelectrons for statistical accuracy reason.

2.3 Data analysis

The first order normalized ACF of a flexible DNA is assumed to be a sum of exponential decays. This is theoretically correct in the small $|K|^2$ scattering vector limit ($|K|^2 \leq 2 \times 10^{14}$

m^{-2}), while at higher $|K|^2$ values it works as a good empirical approximation [13,14]. The second order autocorrelation function $G^{(2)}(t,K)$ used to fit experimental data is therefore:

$$G^{(2)}(t) = A\left\{1 + \left[\sum_{i=1}^{n_{max}} B_i \, e^{-\Gamma_i t}\right]^2\right\} \quad (1)$$

where A is a normalization factor, B_i and Γ_i are the ith pre-exponential factor and relaxation rate, respectively. The nonlinear least-squares fitting program based on the Harwell (C. Urbanke and J. Greipel, unpublished data) subroutine VA05A was kindly provided by J. Langowski. The fitting criterium is the minimum χ^2 and the visual analysis of the residuals. For $|K|^2 \leq 2.3 \times 10^{14}$ m^{-2} ($\vartheta \leq 70°$) a single exponential was sufficient in order to fit the experimental ACFs, while at larger $|K|^2$ values a double exponential function was necessary. In spite of the use of an electronic "dust" filter the introduction of a slow component was necessary when fitting the ACFs. Measurements were performed, for each P_N plasmid, on three or more samples at 0.8×10^{14} $m^{-2} \leq |K|^2 \leq 6.0 \times 10^{14}$ m^{-2}. Furthermore the nicked form of the P_6 plasmid (P_{6n}) has been studied under the same conditions.

3. Results

As suggested in previous works [15,13], a forced single exponential fit performed as preliminary analysis of the data yields the relaxation rate Γ_{app}. The quantity $D_{app} = \Gamma_{app}/|K|^2$ is plotted in Fig. 1. From the extrapolation of this plot to $|K|^2 \cong 0$ it is possible to obtain the translational diffusion coefficient D_t [15,16]. On the other hand the behaviour at high $|K|^2$ value yields hints on the non-translational motions [13]. However, this analysis does not seem applicable to our data since extrapolation to low $|K|^2$ values is not easy due to "dust" contamination affecting data collected at small angles. On the other hand the largest $|K|^2$ available is not large enough to reach the plateau of D_{app} where the contribution of the internal motions is relevant [13].

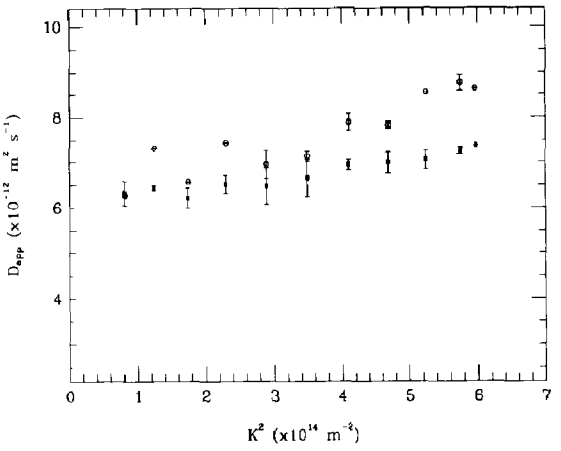

Fig. 1. Apparent diffusion coefficient D_{app} versus $|K|^2$ for P_2 (○) and P_t (■) plasmids.

Therefore we have fitted the ACFs with a double exponential. As already discussed the data are well fitted by a single exponential up to $|K|^2 \cong 2 \times 10^{14}$ m^{-2} while for higher $|K|^2$ values a second component is necessary in order to minimize χ^2 and to avoid correlations in the residuals. The relaxation rates Γ_1 and Γ_2 of the two exponentials are plotted in Fig. 2 and Fig. 3 for plasmid P_1.

From the slope of Γ_1 versus $|K|^2$ the translational diffusion coefficient D_t [17] can be estimated within 1–3% (Table 1), and this is more accurate than the value obtained from the preliminary analysis of the D_{app} plot (see Fig. 1). The

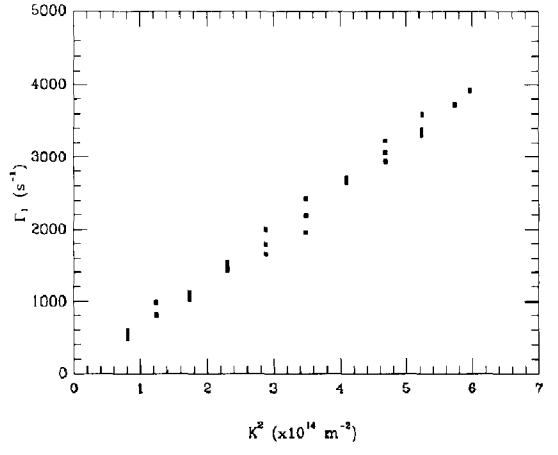

Fig. 2. Relaxation rate Γ_1 versus $|K|^2$ for P_1 plasmid.

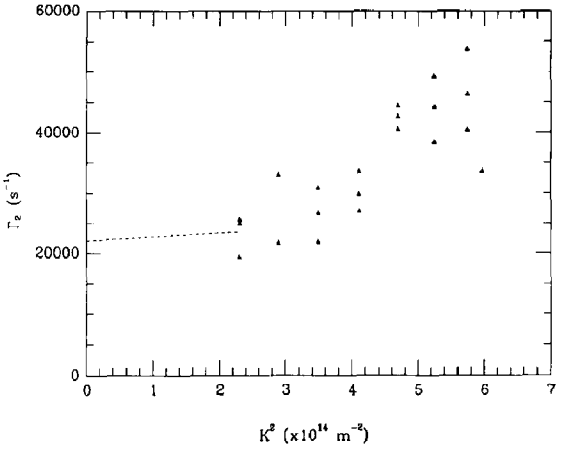

Fig. 3. Relaxation rate Γ_2 versus $|K|^2$ for P_1 plasmid.

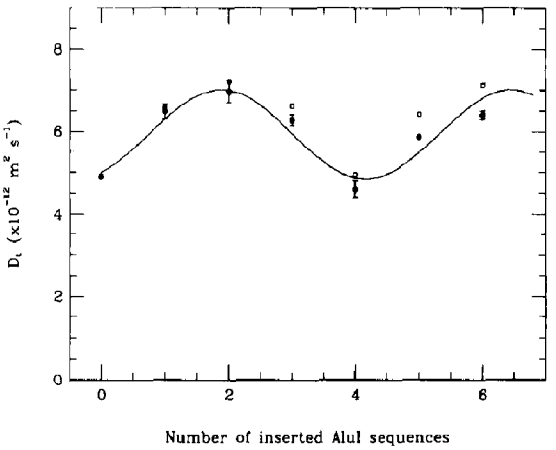

Fig. 4. The translational diffusion coefficients D_t (●) for the whole series of P_N plasmids ($N = 0,\ldots,6$) versus the number of inserted AluI sequences. The symbol (□) refers to mass corrected D_t values. A sinusoidal fit of the experimental data is drawn in order to point out a seemingly periodic trend.

translational diffusion coefficients D_t data from Table 1 are plotted in Fig. 4 versus the number of inserted AluI sequences together with the value of D_t for pUC8 plasmid [13]. This plasmid is assumed as a reference, P_0, when considering the P_N plasmids data, since pUC18m samples suitable for DLS measurements were not available. The number of base pairs in P_0 = pUC8 is 2717, approximately 1% more than pUC18m, and the correspondent error in D_t ($\cong 0.6\%$) is within the experimental uncertainty.

The relaxation rate Γ_2 has been obtained from fits at $|K|^2 > 2.3 \times 10^{-14}$ m^{-2}. As an example we report in Fig. 5 the plot of Γ_2 for the native plasmid P_6 and the nicked P_{6n}. In the case of P_{6n} the behaviour of Γ_2 can be fitted with a linear law

$$\Gamma_2 = D_0 |K|^2 + \Gamma_r \qquad (2)$$

where $D_0 \cong D_t$ and Γ_r is related to the molecular rotational times [18]. Through this analysis it is therefore possible to extrapolate Γ_2 to vanishingly $|K|^2$ values and obtain $\Gamma_r = 10000 \pm 2000$ in good agreement with the same quantity measured

Table 1

Experimental values of diffusion coefficents

P_n	D_t [a]
P_0	4.90 [b]
P_1	6.49 ± 0.18
P_2	6.97 ± 0.27
P_3	6.28 ± 0.13
P_4	4.60 ± 0.20
P_5	5.87 ± 0.20
P_6	6.40 ± 0.10
P_{6n}	5.50 ± 0.015

[a] D_t is in 10^{-12} m^2 s^{-1} units at the temperature of 25°C and the uncertainties correspond to an average over at least three different measurements.

[b] From ref. [13].

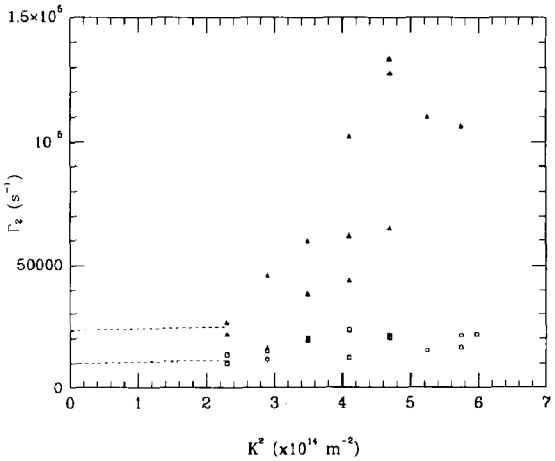

Fig. 5. Relaxation rates Γ_2 versus $|K|^2$ for P_6 (△) and nicked P_{6n} (□) plasmid. Dashed lines are obtained as described in the text.

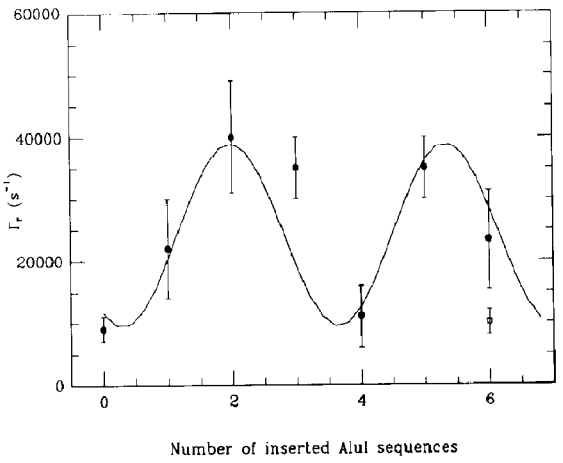

Fig. 6. Rotational rate Γ_r versus number of inserted AluI sequences. A sinusoidal fit of the experimental data is reported in order to make a comparison of Γ_r with the D_t data of Fig. 4. The open square refers to nicked P_{6n} plasmid.

by Langowski [13] for P_0. For the native plasmids, instead, an extrapolation of Γ_2 to low $|K|^2$ is critical [14]. This is due to large uncertainties in Γ_2 and to the non-linear behaviour of Γ_2 in the explored range of $|K|^2$ probably caused by increasing internal motions contributing to the ACF at larger $|K|^2$. An estimate, Γ_r (see Figs. 3 and 5), of Γ_2 at $|K|^2 = 0$ can be obtained by drawing a straight line with D_t slope passing through Γ_2 at the lowest measured $|K|^2$ (Fig. 6). The observed increase in Γ_r for the whole series of plasmids is consistent with the change measured for D_t taking into account the approximate R^{-1} dependence of D_t and the R^{-3} dependence of Γ_r, where R is some typical linear dimension of the molecule.

4. Discussion

Two points are noteworthy. First, the change of D_t upon AluI insertion is not monotonic versus the number of the inserted AluI fragments. The D_t values of P_0 and P_4 are close and the same occurs for P_2 and P_6. When corrections are made in order to take into account that the plasmid mass change with the insertions as described in reference [19], a coincidence of values is found (Fig. 4). The behaviour of D_t versus the number of insertions (Fig. 4) seems to be periodic with a repetition of about four AluI fragments. The striking feature of Fig. 4 is the coincidence of the D_t values for the control plasmid P_0 and the plasmid containing four adjacent AluI sequences (P_4), in spite of the large D_t value reached by P_2 and P_6.

In order to try a rationalization of such a periodic behaviour, some correlations can be pointed out. Electrophoretic and electron microscopy studies [10] suggest for AluI a stable sequence specific curvature with increasing distortion versus the number of inserted AluI units. In particular when the trimer (three AluI sequences) is observed by electron microscopy a C-shaped structure is found, whereas a circular form is reported for the hexamer. These observations suggest a curvature of AluI such that the dimer has a hemicircular shape, the tetramer has a circular shape and so on, as sketched in Fig. 7. These structures nicely correlate with the electrophoretic anomalous K-factor measured by Benfante et al. [10] which reaches a plateau after $N \cong 3$–4. We further observe that the angle between the vectors tangent to the fragment axis at its two opposite ends (dashed lines in Fig. 7), shows a clear "correlation" with the periodic behaviour of D_t. In fact dimer and hexamer show the highest, while the tetramer shows the lowest total curvature. Therefore the apparent periodic behaviour in D_t seems to be closely correlated

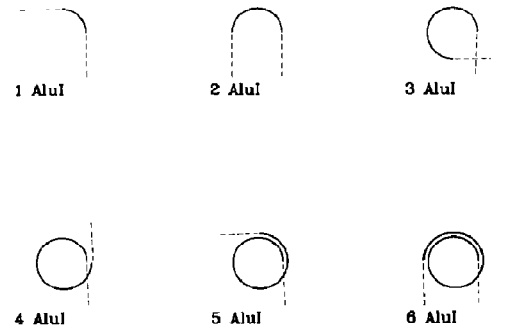

Fig. 7. Conformation of the sequences composed of N contiguous AluI fragments ($N = 1,\ldots,6$). Dashed lines simulate the joint to the host plasmid.

with the number of the curved fragments inserted in the plasmid.

Second, there is a remarkable DNA compaction which seems to be related with the insertion of two or six curved sequences (AluI). The P_0 plasmid shows a translational diffusion coefficient $D_t \cong 30\%$ lower than the plasmids containing two and six AluI sequences. The estimates of the rotational rate Γ_r, although affected by large uncertainties, seem to be in agreement with the observed trend of D_t (see Figs. 4 and 6). The other plasmids display values of D_t lying between those of P_0 and P_2. We therefore focus on the two extreme behaviours, those of the control plasmid P_0 and of the plasmid P_2 containing two AluI sequences.

Studies on plasmids by dynamic light scattering [19] and electron microscopy [20–22] have shown evidence of interwound structure where two DNA double strands are wound around each other to form a more or less rod-like double spiral terminated by loops. The starting point of the data analysis has been therefore the assumption of a linear interwound form. We have computed D_t for such structure and compared the results with the experimental values. We have made use of a known hydrodynamic formula in order to compute the friction coefficient of a "string of beads" as described in the following. The closed DNA is modelled as a string of touching beads of diameter $2\sigma \simeq 3.184$ nm $= (\frac{3}{2})^{0.5} \times 2.6$ nm as suggested by Hagermann [23]. The number N of beads is chosen such as $2\sigma N = L_c$, where L_c is the DNA contour length computed from the base pairs number N_{bp} by the relation $L_c = N_{bp} \times 0.34$ nm. The D_t value is then computed from the De Haen expression [24]:

$$D_t = \frac{k_B T}{6\pi\eta\sigma N}\left[1 + N^{-1}\sum_{i\neq j}^{N} f(x_{i,j})\right]$$

$$f(x) = x - \tfrac{7}{4}x^4 + \tfrac{9}{8}x^6 + \tfrac{13}{2}x^7 + \tfrac{8}{3}x^8 + \tfrac{3}{4}x^9 - \tfrac{167}{6}x^{10} \qquad (3)$$

$$x_{i,j} = \frac{\sigma}{|r_i - r_j|}$$

where k_B, η and T are the Boltzmann constant, the solvent dynamic viscosity and the solution temperature, respectively.

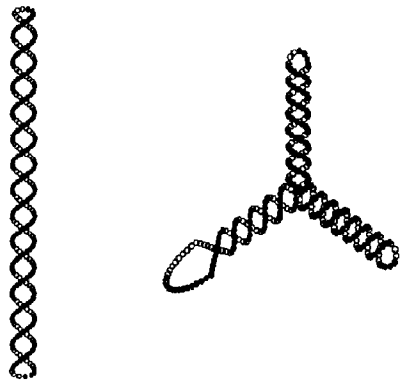

Fig. 8. An example of linear and branched interwound structures used for the D_t simulations.

The simplest interwound structure is assumed to be a linear supercoiled rod where the DNA winds in a right-handed helix up and down the surface of an imaginary cylinder with hemispherical caps on each end (Fig. 8). The one of larger diameter simulates the structure of two AluI sequences (Fig. 7). Each DNA molecule is therefore characterized by the number of supercoils τ (i.e. the number of helical turns about the cylinder), the contour length L_c and the cylinder diameter d.

Values of D_t for the reference plasmid P_0 ($L_c = 923.8$ nm) and for the fastest diffusing plasmid P_2 ($L_c = 990.08$ nm) are reported in Table 2

Table 2

Estimated diffusion coefficients for linear structures

d [c]	P_0 [a] D_t [d]	P_2 [b] D_t [d]
11.0	4.76	5.7
12.0	4.77	6.8
12.2	4.78	7.2
13.0	4.88	14.7
14.0	5.00	– [e]

[a] $\tau = -14$, $n_{nb} = 2717$.

[b] $\tau = -21.8$, $N_{nb} = 2912$.

[c] d is in nm units.

[d] D_t values computed from eq. (3) for an interwound linear form. D_t is in 10^{-12} m^2 s^{-1} units.

[e] No interwound structure is compatible with the geometrical parameters of P_2 for $d = 14.0$ nm.

as a function of d, taking $\tau = -14$ for P_0 [12] and $\tau = -21.8$ for P_2 according to recent data [25]. The predicted D_t is in agreement with the experimental findings for P_0 if one takes the superhelix diameter $d \cong 13$ (± 1) nm. In order to obtain a value of D_t in agreement with the experimental value for P_2 one must assume $d \cong 12.1$ nm. Both the plasmids seem to be described by an interwound form. We recall also that the superhelix geometrical parameters (e.g. the pitch angle α) are bounded by fixed limits according to a simple theoretical approach by Camerini-Otero and Felsenfeld [26] which have shown that $45° \leq \alpha \leq 54°$. Looking at the α value for P_0 and P_2, it easy to realize that P_0 falls nicely within the limits, $\alpha \cong 50°$, while for P_2 $\alpha \cong 21° \pm 2°$. We notice also that the theoretical α limits [26] are not related to any specific choice of the DNA bending or twisting rigidities.

Summarizing, from the above results the simple interwound model employed here appears suitable to describe the conformation of the reference plasmid P_0 in solution. For the plasmids P_2 and P_6, instead, the experimental D_t values clearly indicate a significant compaction of the structure, which cannot be predicted in terms of the simple linear interwound form due to the low α value. Furthermore some electron microscopy works have shown evidence of branched interwound structures with three or more arms. Boles et al. [22] observed a percentage of about 90% of branched form in two derivatives of pBR322 (pAB7.0d with 6978 bp and pJB3.5d with 3480 bp). Laundon and Griffith [27] have studied native pBR325 and two derivatives of the same plasmid ($\simeq$ 6000 bp) finding 63% of the molecules in the branched form. The plasmids used by these authors contained highly curved DNA from *Crithidia Fasciculata* cloned in two pBR325 sites. Laundon and Griffith have also demonstrated an increase of branched structures in the plasmids containing curved sequences and a clear correlation between the position of the curved sequences and the structure of the branched form. In particular the distance between two loops of a branched structure was very similar (within $\simeq$ 2%) to the curved sequences distance in the plasmid map. This fact is taken by the authors as an evidence of the preferential position of the curved sequences at the loops of the interwound structure and is correlated with a higher fraction of supercoiled branched forms. It should be added also that the paper by Boles et al. shows a high percentage (90%) of branched structures but an essentially random location of the branch ends. These results seem to suggest that at least for P_2, the AluI fragment takes the place of one terminating loop: the *Crithidia Fasciculata* fragment used by these authors is remarkably similar in length to two AluI sequences [27]. It appears, however, that the diameter of the loop, as estimated from the base pair number (226 for AluI), is $d \simeq 49$ nm, approximately four times as large as the interwound diameter obtained in this work and from the data by Boles et al. [22].

In order to verify whether and to what extent a branched structure may be suitable to predict the unusual D_t values for P_2 and P_6, we have computed D_t for planar branched interwound structures composed, for sake of simplicity, of three arms of equal length. Each arm is modelled as an interwound segment, one of them is terminated by two AluI adjacent sequences (Fig. 7) and the angle between the arms is assumed to be the same (Fig. 8). The structure is again determined by the arm diameter d, the superhelical turns τ, and the contour length L_c. The results for the P_2 plasmid are displayed in Table 3 for $\tau = -21.8$, as measured in Ref. [25]. We observe that a diameter $d \cong 11.2$ nm yields a $D_t \simeq 6.9 \cdot 10^{-12} m^2 s^{-2}$ in good agreement with the experimental value. The diameter value is consistent with previous experimental studies [22], while the

Table 3

Estimated diffusion coefficients for branched structures

d [a]	D_t [b]	H_1 [c]
11.4	7.2	64
11.2	6.9	69
11.0	6.7	75
10.8	6.5	79

[a] d is in nm units.

[b] D_t values computed from eq. (3) for a three-arms branched interwound form. D_t is in 10^{-12} m^2 s^{-1} units.

[c] H_1 is the arm length in nm units.

corresponding helical pitch angle $\alpha \simeq 30° \pm 1°$ is below that predicted ($45° \leq \alpha \leq 54°$) [26] for the linear interwound form. However, in our branched structure the choice of uniform interwound arms (uniform pitch and radius) takes into account more the geometry than the internal elastic stress of the branch point. Therefore the pitch values estimated for the branched form cannot be retained as reliable as those given here for the linear interwound structure. The estimate of the structure deformation due to the branch point would need Monte Carlo simulations of the supercoiled conformation which are under development in our laboratory.

5. Conclusions

Dynamic light scattering studies of a series of plasmids, derived from pUC18m, each containing a different repetition number of the curved sequence AluI, show that these plasmids may adopt highly compact structures in solution. An open question remains about the non-monotonic behaviour of the degree of compaction, expressed by the reciprocal of the translational diffusion coefficient, versus the amount of AluI insertion. Such a behaviour is confirmed also by the rotational diffusion rate Γ_r measured on the same plasmids.

In summary, we have shown the existence of a correlation between the structure of the AluI inserted sequences and the value of D_t and Γ_r for the corresponding host plasmids. Since the AluI sequence appears with a high repetition number in the *Artemia Franciscana* heterochromatin, the observed non-monotonic behaviour may play an interesting role in the heterochromatin organization. Furthermore, the observed compaction of the plasmids containing certain amount of AluI sequences, may be brought as evidence of the organizing role of this part of the chromatin.

Acknowledgements

This research has been partially supported by Centro Interuniversitario di Struttura della Materia. Thanks are due to G. Badaracco for providing the plasmids used in the present research and for useful stimulating discussions. We gratefully acknowledge also Ulrike Kapp for sample preparation, Lorenzo Lunelli for helpful suggestions and Marco Gardella for technical assistance.

References

1 W.C. Earnshaw, Current Opinion Struct. Biol. 1 (1991) 237.
2 H. Echols, Science 233 (1986) 1050.
3 J. Widom, Current Opinion Struct. Biol. 1 (1991) 245.
4 W.R.Mc. Clure, Annu. Rev. Biochem. 54 (1985) 171.
5 J.B. Bliska and N.R. Cozzarelli, J. Mol. Biol. 194 (1986) 205.
6 E.N. Trifonov, CRC Crit. Rev. Biochem. 19 (1985) 89.
7 H.A. Nash, TIBS 15 (1990) 222.
8 R.B. Lobell and R.F. Schleif, Science 250 (1990) 528.
9 C. Barigozzi, G. Badaracco, P. Plevani, L. Baratelli, S. Profeta, E. Ginelli and R. Menerveri, Chromosoma (Berlin) 90 (1984) 332.
10 R. Benfante, N. Landsberger, G. Tubiello and G. Badaracco, Nucleic Acids Res. 17 (1989) 8273.
11 S. Diekman, Nucleic Acid and Molecular Biology, eds. F. Eckstein and D. Lilley (Springer-Verlag, Berlin, 1987) p. 138.
12 J. Langowski, W. Kremer and U. Kapp, in: Methods in Enzimology, 211: DNA Structure, eds. D. Lilley and J. Dahlberg (Springer-Verlag, Berlin, 1992) in press.
13 J. Langowski, U. Giesen and C. Lehmann, Biophys. Chem. 25 (1986) 191.
14 G. Chirico and G. Baldini, J. Mol. Liq. 41 (1989) 327.
15 K. Soda and A. Wada, Biophys. Chem. 20 (1984) 185.
16 S.C. Lin and J.M. Schurr, Biopolymers 17 (1978) 425.
17 M. Caloin, B. Wilhelm and M. Daune, Biopolymers 16 (1977) 2091.
18 R. Pecora, J. Phys. Chem. 69 (1968) 1036.
19 J. Langowski and U. Giesen, Biophys. Chem. 34 (1989) 9.
20 J. Vinograd, J. Lebowitz, R. Radloff, R. Watson and P. Laipis, Biochem. 53 (1965) 1104.
21 W.B. Upholt, H.B. Gray and J. Vinograd, J. Mol. Biol. 61 (1971) 21.
22 T.C. Boles, J.H. White and N.R. Cozzarelli, J. Mol. Biol. 213 (1990) 931.
23 P.J. Hagerman and B.H. Zimm, Biopolymers 20 (1981) 1481.
24 C. De Haen, R.A. Easterly and D.C. Teller, Biopolymers 22 (1983) 1133.
25 M. Collini, L. Lunelli, G. Chirico, G. Baldini and G. Badaracco, in: SIF; Conf. Proc. 31; Cybernetics and Biophysics Italian Conference, ed. C. Frediani (Editrice Compositori Bologna 1991) p. 89; and M. Collini, personal communication.
26 R.D. Camerini-Otero and G. Felsenfeld, Proc. Natl. Acad. Sci. USA 75 (1978) 1708.
27 C.H. Laundon and J.D. Griffith, Cell 52 (1988) 545.